Perpendicular giant magnetoresistance and magnetic switching properties of a single spin valve with a synthetic antiferromagnet as a free layer

Y. Jiang, S. Abe, T. Nozaki, N. Tezuka, and K. Inomata
Department of Materials Science, Graduate School of Engineering, Tohoku University, Sendai 980-8579, Japan
and CREST, Japan Science and Technology Corporation, Kawaguchi, Saitama 332-0012, Japan
(Received 18 July 2003; revised manuscript received 23 September 2003; published 24 December 2003)

We study the current-perpendicular-to-plane giant magnetoresistance (CPP-GMR) and magnetic switching behavior of single spin-valve (SV) films with two different free layers—one is a single ferromagnet (FM) layer, while the other is a synthetic antiferromagnet (SyAF) consisting of $Co_{90}Fe_{10}$/Ru/$Co_{90}Fe_{10}$. When the interlayer Cu thickness is 2.5 nm, the SyAF as a free layer greatly enhances the CPP-GMR of SVs from 0.8% to 3.6%. The GMR enhancement effect decreases with increasing interlayer Cu thickness. We argue that the MR enhancement by the SyAF is probably because of strong reflection of the majority spins by the interface between $Co_{90}Fe_{10}$ and ruthenium. Experimental and theoretical studies of the magnetic switching behavior show that the SVs with SyAF have a much better tendency to form a single magnetic domain than the conventional ones. The single domain structure results in a size-independent magnetic switching field of the SVs with SyAF at the low aspect ratio 1.

DOI: 10.1103/PhysRevB.68.224426 PACS number(s): 75.47.De, 75.70.Kw, 72.25.Ba

I. INTRODUCTION

There has been great interest in multilayers composed of alternating ferromagnetic (FM) and nonmagnetic metal (N) layers since the discovery of giant magnetoresistance (GMR) in this system.[1] Introduction of a GMR read head to the hard disk drive stimulated substantial increase of the drive capacity.[2] All present GMR-based devices are with current-in-plane (CIP) geometry, i.e., the sensing current flows in the plane of the multilayers. There is another even more interesting GMR effect that was found in CPP geometry in the 1990s,[3] i.e., the sensing current flows perpendicular to the plane of the mutilayers. The amplitude of CPP-GMR is usually higher than that of CIP-GMR. Thus CPP-GMR is hopefully one of the best candidates as the next generation magnetic head material used in ultrahigh density hard disks.[4] The CPP-GMR becomes more competitive when the device size shrinks because of the large output voltage signal. On the other hand, in order to control the domain structure and decrease coercivity, a spin-valve (SPV or SV) structure is usually used instead of a multilayer as the magnetic read head.[5] The interfaces between FM and N layers in SVs are far fewer than those in a multilayer, so the CPP-GMR of SPVs is much smaller than that of multilayers. The too low resistance (R) and MR of conventional CPP-GMR SVs prevents its direct usage as a magnetic read head. On the other hand, it is still difficult to control the domain structure of SVs, especially when its size shrinks to the submicrometer or nanometer scale because of a large demagnetizing field arising from the poles at the edges of elements, and leading to a complex domain structure which depends on the aspect ratio of the elements. A higher aspect ratio causes a large magnetic switching field, while a low aspect ratio induces a multidomain structure, which hampers the development of ultrahigh density magnetic recording. In previous works,[6] we studied the domain configuration of a synthetic antiferromagnetic (SyAF) structure consisting of antiferromagnetically coupled FM layers sandwiched by a N layer. The SyAF structure allows an enclosed magnetic flux and creates less stray field, which reduces the magnetostatic coupling with the closely neighboring FM layer, and facilitates the formation of a single domain even when the aspect ratio is 1. In this paper, we apply the SyAF structure in a CPP-GMR SV as a free layer and demonstrate that SyAF as a free layer dramatically enhances the CPP-GMR, and improves the magnetic switching behavior of CPP SVs. The possible mechanisms of these improvements are discussed.

II. EXPERIMENT

Our CPP-GMR SV structure is Cu(20 nm)/IrMn(10 nm)/$Co_{90}Fe_{10}$(3 nm) / Cu(d nm) / free layer / Cu(5 nm)/Ta(2 nm). Two kinds of free layer are used. One is a single $Co_{90}Fe_{10}$ film with a thickness of 5 nm and the other is a SyAF structure of $Co_{90}Fe_{10}$(5 nm)/Ru(0.45 nm)/$Co_{90}Fe_{10}$ (3 nm). Here we label the samples with a single $Co_{90}Fe_{10}$ free layer ''conventional CPP-GMR'' and those with SyAF ''CPP-GMR with SyAF.'' The interlayer Cu thickness d ranges from 2.5 nm to 6 nm. Our fabrication process is ''subtractive.'' The multilayer was first deposited on a Si/SiO_2 substrate in an ultrahigh vacuum sputtering system with a base pressure below $\sim 5\times 10^{-9}$ Torr. A 200 Oe magnetic field was applied during the sputtering in order to induce an easy axis. Then the bottom electrode Cu and top electrode Cu/Ta were patterned using electron beam lithography and subsequent ion milling etching. After this, the GMR SPV element was etched out followed by SiO_2 sputtering. A thick capping layer of Cu was then coated using the lift-off process. A schematic cross section view of the fabricated CPP-GMR element is shown in Fig. 1(a), where the element size A is clearly defined. As shown in Fig. 1(b), the shape of all elements is rectangular, with a length l and width w. The aspect ratio k is defined as $k=l/w$. The size A of elements varies from 4×1 μm^2 to 0.2×0.2 μm^2. Four-probe measurements of transport properties were carried out in CPP geometry at

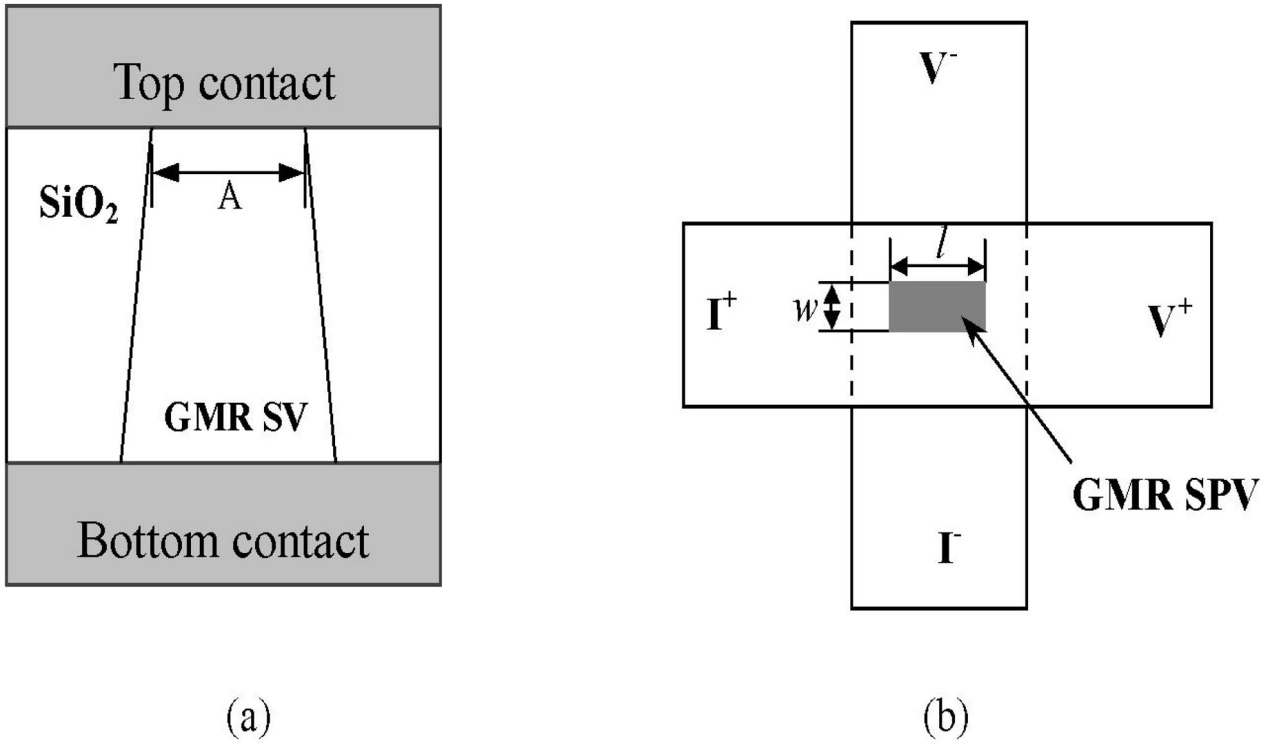

FIG. 1. The (a) cross section and (b) top view of the fabricated CPP-GMR element. The element's size is defined as *A*.

room temperature with magnetic fields applied along the easy axis as shown in Fig. 1(b). The easy axis direction is along the length of the elements. The measuring current was kept below ~1 mA to avoid any other effect induced by the current.

III. RESULTS AND DISCUSSION

A. CPP-GMR enhancement by SyAF

The magnetization curves of CPP-GMR with SyAF SVs were measured. The results are similar to Fig. 2 of Ref. 7, except for a much higher saturation magnetic field (~12 000 Oe) and a little lower saturation magnetization ($M_S \sim 937$ emu/cm^3), which means a stronger AF coupling in the SyAF structure we used in this study. Then we measured the CPP-GMR of the elements with a fixed interlayer thickness $d=2.5$ nm. The *R*-*H* curves of both the conventional CPP-GMR and CPP-GMR with SyAF elements are shown in Fig. 2. Figures 3(a) and 3(b) show the size dependence of R and the resistance change ΔR for these two kinds of element. R and ΔR are both inversely proportional to A. When we assume an infinite spin-diffusion length and apply the Valet-Fert (VF) model[8] to the conventional CPP-GMR structure, the resistance change–area product $A\Delta R$ is written as[5,10]

$$A\Delta R = \frac{(2\beta\rho^*_{Co_{90}Fe_{10}} t_{Co_{90}Fe_{10}} + 2\gamma AR^*_{Co_{90}Fe_{10}/Cu})^2}{AR_{IrMn/Co_{90}Fe_{10}} + 2\rho^*_{Co_{90}Fe_{10}} t_{Co_{90}Fe_{10}} + \rho_{Cu} t_{Cu} + 3AR^*_{Co_{90}Fe_{10}/Cu}}, \quad (1)$$

where β and γ are the spin asymmetry coefficients of the $Co_{90}Fe_{10}$ layer and $Co_{90}Fe_{10}/Cu$ interface, respectively. The spin-dependent resistivities $\rho^*_{Co_{90}Fe_{10}} = \rho_{Co_{90}Fe_{10}}/(1-\beta^2)$ and $AR^*_{Co_{90}Fe_{10}/Cu} = AR_{Co_{90}Fe_{10}/Cu}/(1-\gamma^2)$. $\rho_{Co_{90}Fe_{10}}$ and ρ_{Cu} are the measured resistance values of $Co_{90}Fe_{10}$ and Cu, respectively. $AR_{Co_{90}Fe_{10}/Cu}$ and $AR_{IrMn/Co_{90}Fe_{10}}$ are the interface resistances. $t_{Co_{90}Fe_{10}}$ and t_{Cu} are the total thickness of all the FM layers and the Cu layers, respectively. In our system, the measured $\rho_{Co_{90}Fe_{10}}$ is 15.4 $\mu\Omega$ cm, ρ_{Cu} is 1.7 $\mu\Omega$ cm. The value of $AR_{Co_{90}Fe_{10}/Cu}$ is 0.22 mΩ μm^2,[9] while $AR_{IrMn/Co_{90}Fe_{10}}$ is approximated as 0.95 mΩ μm^2, which is supposed to be the same as $AR_{FeMn/Co_{90}Fe_{10}}$.[10] Applying $\beta=0.65$ and $\gamma=0.75$, the calculated $A\Delta R$ using Eq. (1) is 1.8 mΩ μm^2, which is shown as the linear line in Fig. 3(a).

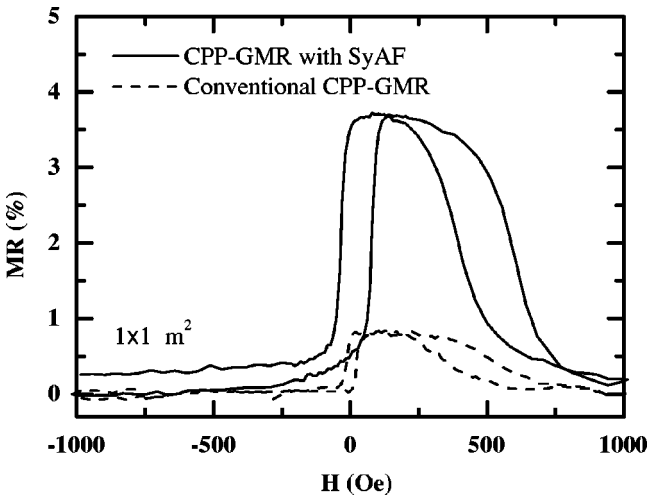

FIG. 2. MR curves of conventional CPP-GMR and CPP-GMR with SyAF elements when the interlayer Cu is 2.5 nm. The size of the elements is $1\times1\ \mu m^2$.

We can see that our experimental results fit well with the VF model calculation. It is noteworthy that our calculation does not include the resistance of bottom and top electrodes. The good agreement between experiment and calculation means negligible contact resistance in our system. In a similar way, the calculated resistance-area product *RA* is around $0.23\ \Omega\ \mu m^2$ for the conventional CPP-GMR. Thus we obtain a MR value of 0.8% for the conventional CPP-GMR structure, which is nearly the same as the previous report on a similar structure.[5] For the CPP-GMR with SyAF structure, as shown in Fig. 3(b), by fitting to the experimental data, we obtain $A\Delta R=16.8\ m\Omega\ \mu m^2$ and $RA=0.47\ \Omega\ \mu m^2$. The MR of CPP-GMR with SyAF is $\sim$3.6%, which is nearly four times higher than that of the conventional one. We think this enhancement is because of the existence of a Ru layer in SyAF structure. According to Campbell and Fert,[11] introducing Ru into Co should lead to a negative magnetic scattering anisotropy, which means that Ru impurities in Co will scatter majority spins more strongly than minority ones. The scattering anisotropy α is defined as the ratio between the resistance of spin-down and spin-up electrons. For Ru impurities in a Co system, α is around 0.22,[11] i.e.,

$$\alpha=\frac{\rho_{0\downarrow}}{\rho_{0\uparrow}}=\frac{1+\gamma_{Co_{90}Fe_{10}/Ru}}{1-\gamma_{Co_{90}Fe_{10}/Ru}}=0.22. \qquad (2)$$

Thus we obtain the interfacial anisotropy parameter $\gamma_{Co_{90}Fe_{10}/Ru}\approx-0.64$. Applying this value and the experimental result $A\Delta R=16.8\ m\Omega\ \mu m^2$ in the VF model, one can easily obtain the spin-dependent interfacial resistivity between the Ru and $Co_{90}Fe_{10}$ layers as $AR^*_{Co_{90}Fe_{10}/Ru}\approx5.19\ m\Omega\ \mu m^2$, which is much higher than $AR^*_{Co_{90}Fe_{10}/Cu}\sim0.5\ m\Omega\ \mu m^2$. This high spin-dependent interfacial resistivity implies strong interfacial spin scattering. We think the MR enhancement by SyAF is because of the strong spin scattering in the interface between Ru and $Co_{90}Fe_{10}$ layers.

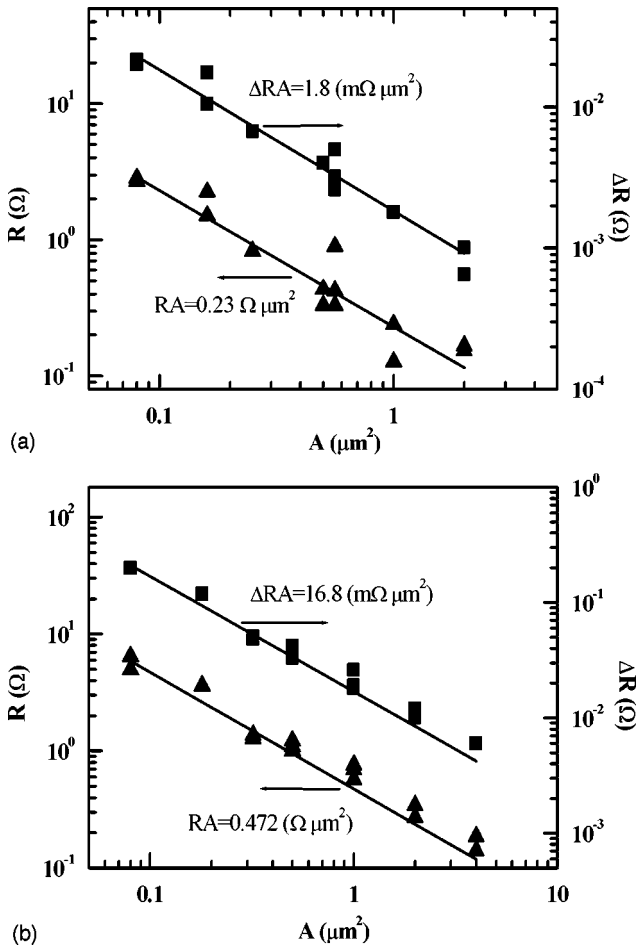

FIG. 3. Resistance *R* and resistance change ΔR as a function of element size *A* for (a) the conventional CPP-GMR and (b) CPP-GMR with SyAF. The solid lines are the calculation results by the VF model.

To further understand the mechanism of MR enhancement by the SyAF free layer, we studied the effect of the interface Cu thickness on the MR enhancement. Conventional CPP-GMR and CPP-GMR with SyAF SVs with different interlayer Cu thickness *d* were fabricated. The measurement results of *RA* and MR are shown in Fig. 4. For the conventional CPP-GMR structure, the interlayer Cu thickness has not so much effect on its MR and *RA*, which can be easily understood using Eq. (1). But for the CPP-GMR with SyAF structure, *RA* greatly increases and MR greatly decreases with increasing interlayer Cu thickness. Such dramatic changes of *RA* and MR possibly originate from the changing interfacial resistivity $AR^*_{Co_{90}Fe_{10}/Ru}$ with Cu thickness. The thicker the interlayer Cu, the farther the spins need to move before they reach the $Co_{90}Fe_{10}/Ru$ interface. This decreases the spin-diffusion length of the electrons and thus weakens the spin scattering at the $Co_{90}Fe_{10}/Ru$ interface. But some other effects should be included. For example, the spins may pass by a much longer way than the total thickness of the multilayers, because they are reflected by both the Ru cap and the AF IrMn layer.

We also studied another SPV structure with a thin Ru cap layer on the free layer. The SPV structure is

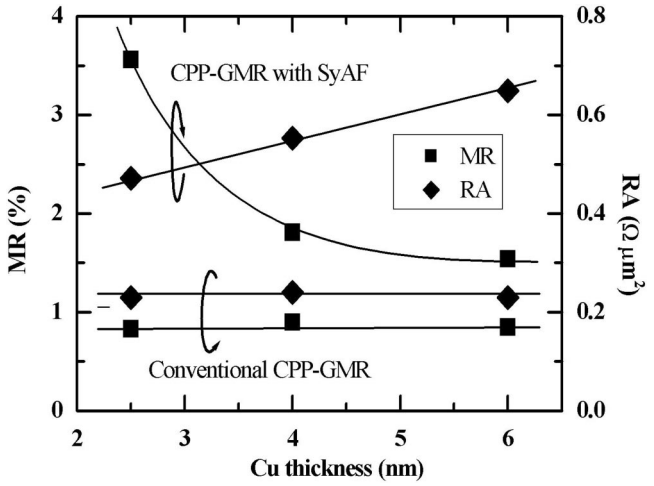

FIG. 4. *R* and MR as a function of interlayer Cu thickness *d* for conventional CPP-GMR and CPP-GMR with SyAF. The solid lines are guides to the eyes.

Cu (20 nm) / IrMn (10 nm) / $Co_{90}Fe_{10}$ (3 nm) / Cu(2.5 nm)/ $Co_{90}Fe_{10}(t_{free})$/Ru(t_{Ru})/Cu(5 nm)/Ta(2 nm). The CPP-GMR of one element ($t_{free}=5$ nm; $t_{Ru}=0.45$ nm) with a designed size 0.1×0.1 μm^2 is shown in Fig. 5. Not surprisingly, we can also get a higher MR value that is around 3.2%. The Ru and free layer $Co_{90}Fe_{10}$ thickness dependences of MR are shown in Figs. 6(a) and 6(b), respectively. With increasing t_{Ru}, the MR has a peak around $t_{Ru}=0.45$ nm. When t_{Ru} is too small, the Ru/FM interface is discontinuous. The reflection effect of the majority spins by the Ru/FM interface is not so strong. For SPVs with too thick Ru, the total resistance is higher, so the MR decreases. When t_{free} increases, the MR increases first and reaches a peak value when $t_{free}=6$ nm. Further increasing t_{free} decreases the MR. For comparison, we also show the result for the conventional structure Cu(20 nm)/IrMn(10 nm)/

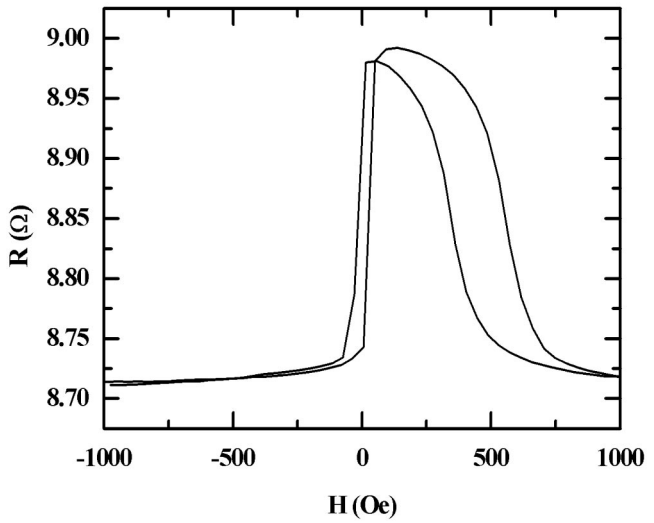

FIG. 5. CPP-GMR curve of a SPV with a designed size 0.1×0.1 μm^2 and structure Cu(20 nm)/IrMn(10 nm)/$Co_{90}Fe_{10}$ (3 nm)/ Cu (2.5 nm)/Co_{90} Fe_{10} (5 nm)/Ru (0.45 nm)/Cu(5 nm)/Ta(2 nm).

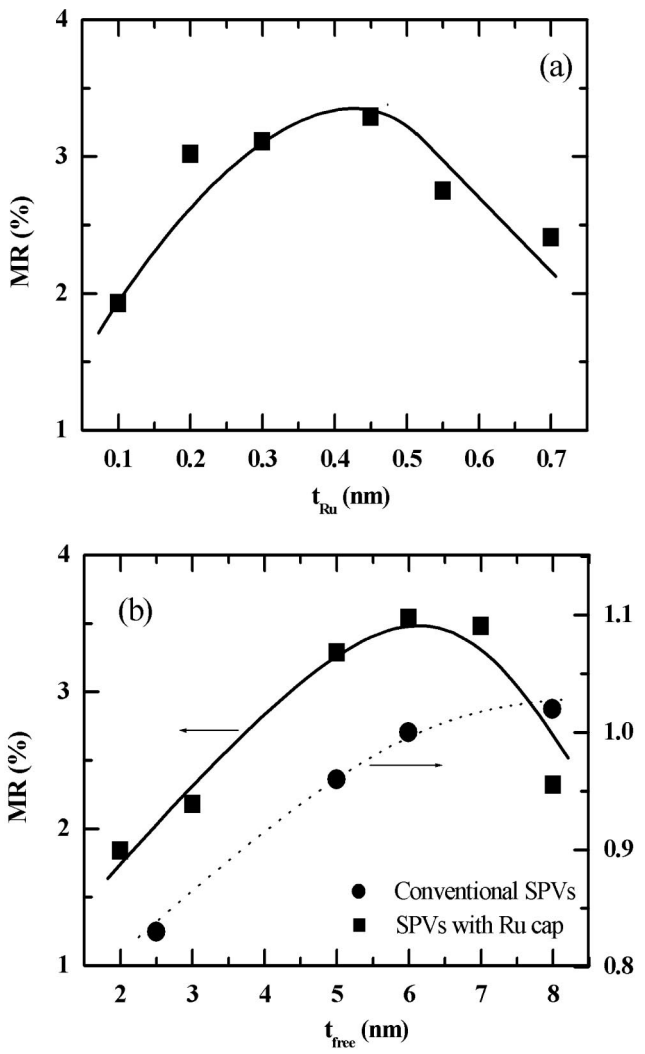

FIG. 6. (a) The Ru thickness dependence of MR for the structure with a Ru cap layer; (b) the free layer thickness dependence of MR for the structure with and without a Ru cap layer.

$Co_{90}Fe_{10}$ (3 nm) / Cu(2.5 nm) / $Co_{90}Fe_{10}(t_{free})$ / Cu(5 nm)/ Ta(2 nm) in Fig. 6(b). For the conventional structure, the MR increase monotonically and no MR peak can be observed when t_{free} is smaller than 8 nm. This is reasonable because 8 nm is still smaller than the spin-diffusion length of the $Co_{90}Fe_{10}$ layer, which is around 12 nm as reported.[9] For the SPVs with a Ru cap layer, we think the ''effective thickness'' of the free layer is much longer than t_{free} because of the reflection of the majority spins by the Ru/FM interface and IrMn layer. Thus we have a MR peak when t_{free} is around 6 nm. This can also help us to understand the result of Fig. 4.

B. Single-domain magnetic switching behavior of CPP-GMR with SyAF

The MR measurement was also carried out under a magnetic field with different sweep rates that change from 0.4 Oe/s to 40 Oe/s. Figure 7 gives the magnetic field sweep-rate-dependent easy axis minor hysteresis loop correspond-

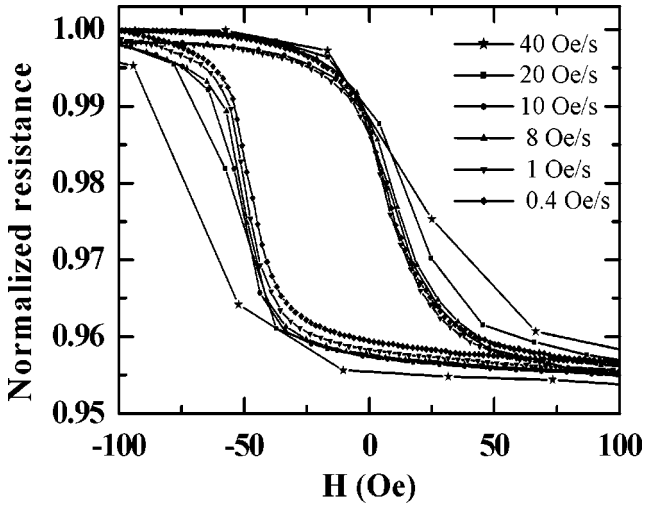

FIG. 7. Sweep-rate-dependent magnetic switching of the free layer for a CPP-GMR with SyAF element with a size of 0.5 $\times 0.5\ \mu m^2$.

ing to the rotation of the free layer of the SV. The SV structure is CPP-GMR with SyAF and the size is 0.5 $\times 0.5\ \mu m^2$. The magnetic switching field (H_{sw}) changes from 82 Oe to 64 Oe, while the field sweep rate changes from 40 Oe/s to 0.4 Oe/s. If the element is of single-domain structure, this phenomenon can be described by a single-domain thermal activation model,[12,13] which gives

$$R_H = \frac{\gamma_0}{2C(H_k - H_{sw})} \exp[-C(H_k - H_{sw})]. \tag{3}$$

Here R_H is the magnetic sweep rate, γ_0 is the attempt frequency (on the order of 10^9 Hz), $C = K/k_B T H_k^2$, $K = 0.5 m H_k$ is the uniaxial anisotropy energy, and H_k is the uniaxial anisotropy field, which can be calculated from

$$H_k = 4\pi M_S \left(\frac{t}{w}\right)(n_y - n_x) + H_u, \tag{4}$$

where

$$n_x = (k/2)\int_0^\infty \frac{ds}{(k^2+s)\sqrt{(k^2+s)(1+s)s}},$$
$$n_y = (k/2)\int_0^\infty \frac{ds}{(1+s)\sqrt{(k^2+s)(1+s)s}}. \tag{5}$$

Here $k = l/w$, l, w, and t are the length, width, and thickness of the film, respectively, and H_u is the intrinsic uniaxial anisotropy field. Here we assume H_u is zero, because the magnetic anisotropy of $Co_{90}Fe_{10}$ is negligible compared with the demagnetization energy.

Now let us use Eq. (3) to fit our experimental results for the relationship between R_H and H_{sw}. We fix γ_0 as 1.23×10^9 Hz, which was proved to be the best value for our fitting. In Fig. 8, we give the field sweep-rate dependence of

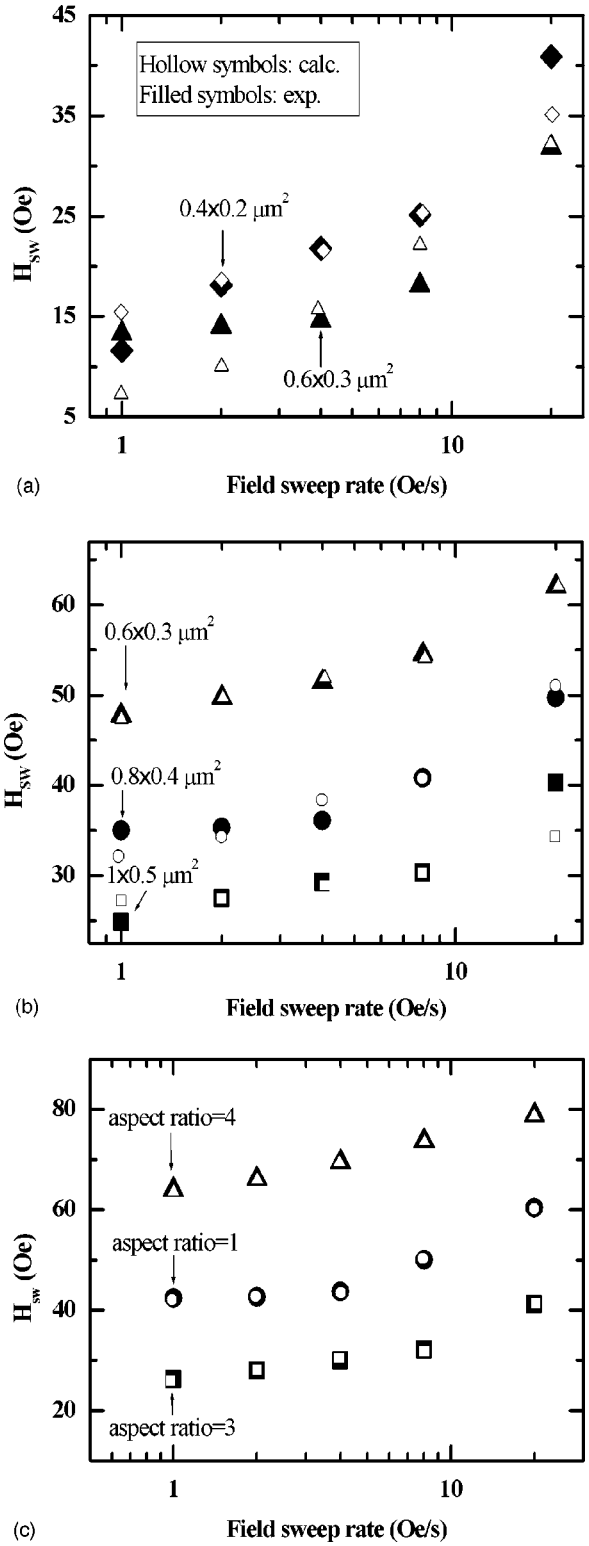

FIG. 8. The field sweep-rate dependence of magnetic switching field for (a) conventional CPP-GMR elements with different sizes, (b) CPP-GMR with SyAF elements with different sizes, and (c) CPP-GMR with SyAF elements with an identical size 0.18 μm^2 but different aspect ratios. The filled symbols are experimental data. The open symbols represent the single-domain model fitting results using Eq. (3). For all the elements, the interlayer Cu thickness is 2.5 nm.

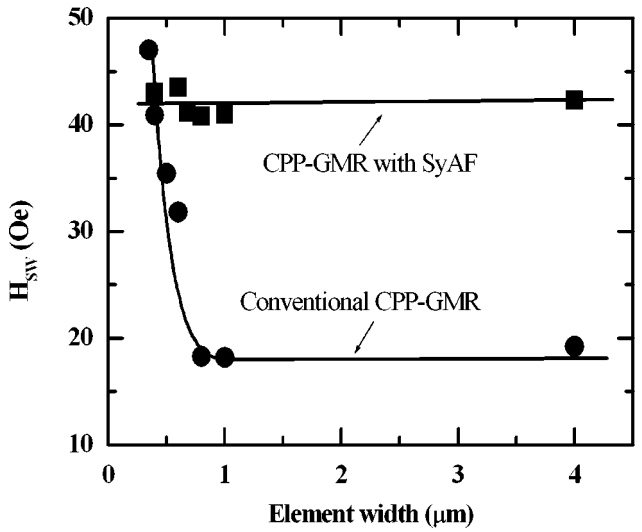

FIG. 9. The magnetic switching field as a function of element width for conventional CPP-GMR and CPP-GMR with SyAF SVs.

the magnetic switching field for the conventional CPP-GMR and CPP-GMR with SyAF elements. The open symbols are the fitting results using Eq. (3). Here the only adjustable parameter is H_k. In Fig. 8(a), for conventional CPP-GMR, its switching behavior is far from the fitting result by the single-domain thermal activation model, even though the element size decreases to as small as $0.4\times0.2\ \mu m^2$. But for CPP-GMR with SyAF, when the element size decreases to around $0.6\times0.3\ \mu m^2$, the variation of H_{sw} under different magnetic field sweep rates fits the single-domain model well, as shown in Fig. 8(b). To exclude a possible effect of the aspect ratio, different aspect ratio elements with constant area $0.18\ \mu m^2$ were also studied. As shown in Fig. 8(c), the observed sweep-rate dependence of H_{sw} shows good agreement with the single-domain model for CPP-GMR with SyAF elements, while their size decreases to $0.18\ \mu m^2$, even with the low aspect ratio of 1.

As we mentioned above, the uniaxial anisotropy field H_k can also be directly calculated by the single-domain model using Eqs. (4) and (5). From the above mentioned magnetization measurement, the moment-thickness products used in our calculation are $M_s t \approx 9.75\times10^{-4}$ emu/cm^2 for the conventional CPP-GMR SV and $M_s t \approx 7.64\times10^{-4}$ emu/cm^2 for the CPP-GMR with SyAF SV with interlayer Cu thickness 2.5 nm. Table I shows a comparison between H_k from fitting and H_k from the single-domain calculation. The relative error between them is also shown in the table.

From Table I, for the conventional CPP-GMR, the large difference between fitted and calculated H_k implies that the single-domain model is not applicable to the structure, when the size is not smaller than $0.4\times0.2\ \mu m^2$. Actually, Sun *et al.* reported a good agreement of single-domain calculation with the experimental result for the conventional structure, when its size is down to $0.1\times0.2\ \mu m^2$.[13] For the CPP-GMR with SyAF, the single-domain model can perfectly explain the magnetic switching behavior, when the element's size diminishes to $0.18\ \mu m^2$, with any aspect ratio. This value ($\sim0.18\ \mu m^2$) is far larger than $0.1\times0.2\ \mu m^2$, which means that the CPP-GMR with SyAF has a much better tendency to form a single domain than the conventional one. This result is consistent with the single-domain observation of SyAF we reported before.[6]

C. Size-independent magnetic switching field of CPP-GMR with SyAF

Under a fixed magnetic field sweep rate 8 Oe/s, we measured the switching field H_{sw} of the conventional CPP-GMR and CPP-GMR with SyAF elements. The aspect ratio of all samples is 1. H_{sw} as a function of element size is shown in Fig. 9, for both structures. The switching field of a conventional CPP-GMR structure substantially increases when the element's width diminishes below 1 μm. This is because a significantly large demagnetizing field of the element arises, when its size decreases to the submicrometer or nanometer scale. As for the CPP-GMR with SyAF, the switching field stays nearly constant with decreasing size. We noted that this size-independent magnetic switching field can be observed only in the element with aspect ratio 1.

As reported, for a single-domain structure, the switching field of SyAF with strong enough AF coupling can be written as[14]

$$H_{sw}=\frac{2K_u(t_1+t_2)}{M_1t_1+M_2t_2}+C(k)\frac{M_1t_1+M_2t_2}{w}, \qquad (6)$$

where K_u is the uniaxial magnetic anisotropy of the magnetic layer, M_i and t_i $(i=1,2)$ are the magnetization and thickness

TABLE I. Comparison between fitted and calculated values of H_k.

$l\times w$ (μm^2)	Conventional CPP-GMR			CPP-GMR with SyAF		
	H_k (Oe) Fitted	H_k (Oe) Calculated	Error(%)	H_k (Oe) Fitted	H_k (Oe) Calculated	Error (%)
0.8×0.4	598	173.7	−70.95	222.5	108.6	−51.2
0.8×0.2				400	401.6	+0.4
0.72×0.24				291.5	292.4	+0.3
0.6×0.3	458	231.6	−49.4	180.4	181.5	+0.066
0.5×0.25				198	136	−31.3
0.42×0.42				84		
0.4×0.2	244	347.3	+42.3	267.3	272	+1.8

of the magnetic layer *i*, respectively, and $C(k)$ is the demagnetizing factor, which is dependent on the aspect ratio *k*. The first term is the uniaxial magnetic anisotropy field and the second one is the demagnetizing field. When the element width *w* is large, the second term is negligible. H_{sw} is given by the first term and thus is size independent. When the element width *w* becomes small enough, the second term becomes dominant and H_{sw} increases with decreasing *w*, which has been observed in SyAF with an aspect ratio $k \neq 1$.[14] In the special case $k=1$, $C(k)=0$,[15] so the second term of Eq. (6) is zero. H_{sw} is independent of *w*. Thus the size-independent switching field of CPP-GMR with SyAF benefits from the strong AF coupling in SyAF and the single-domain magnetic structure at the low aspect ratio 1.

IV. SUMMARY

In this paper, both conventional CPP-GMR and CPP-GMR with SyAF SVs are studied. SyAF as a free layer dramatically enhances the room temperature CPP-GMR from 0.8% to 3.6% when the interlayer Cu thickness is 2.5 nm. The MR enhancement effect decreases with increasing interlayer Cu thickness. The study of SPVs with a Ru cap layer demonstrates that the MR enhancement by a SyAF or single Ru cap layer is because of the large interfacial spin scattering between Ru and $Co_{90}Fe_{10}$ layers. Experimental and theoretical studies of the magnetic switching behavior demonstrate that the CPP-GMR with SyAF shows single-domain switching behavior, when the element size decreases down to 0.18 μm^2 with any aspect ratio. The strong AF coupling and single domain of SyAF result in a size-independent magnetic switching field for the CPP-GMR with SyAF element under aspect ratio 1. The CPP-GMR with SyAF structure has great potential to be used in future ultrahigh recording density storage.

ACKNOWLEDGMENT

One of us (Y.J.) thanks J. Z. Sun (IBM Research) for helpful discussions about the single-domain thermal activation model calculations. This work was supported by the IT program of Research Revolution 2002, the Priority Area 1407602 from NEXT, and a NEDO grant for the NAME and SCAT.

[1] M.N. Baibich, J.M. Broto, A. Fert, F.N.V. Dau, F. Petroff, P. Etienne, G. Creuzet, A. Friederich, and J. Chazelas, Phys. Rev. Lett. **61**, 2472 (1988); W.J. Gallagher, S.S.P. Parkin, Y. Lu, X.P. Bian, A. Marley, R.A. Altman, S.A. Rishton, K.P. Roche, C. Jahnes, T.M. Shaw, and G. Xiao, J. Appl. Phys. **81**, 3741 (1997).

[2] E. Grochowski and R.D. Halem, IBM Syst. J. **42**, 338 (2003).

[3] W.P. Pratt, Jr., S.-F. Lee, J.M. Slaughter, R. Loloee, P.A. Schroeder, and J. Bass, Phys. Rev. Lett. **66**, 3060 (1991).

[4] M. Takagishi, K. Koi, M. Yoshikawa, T. Funayama, H. Iwasaki, and M. Sahashi, IEEE Trans. Magn. **38**, 2277 (2002).

[5] H. Yuasa, M. Yoshikawa, Y. Kamiguchi, K. Koi, H. Iwasaki, and M. Takagishi, J. Appl. Phys. **92**, 2646 (2002).

[6] N. Tezuka, N. Koike, K. Inomata, and S. Sugimoto, Appl. Phys. Lett. **82**, 604 (2003).

[7] K. Inomata, T. Nozaki, N. Tezuka, and S. Sugimoto, Appl. Phys. Lett. **81**, 310 (2002).

[8] T. Valet and A. Fert, Phys. Rev. B **48**, 7099 (1993).

[9] J. Bass and W.P. Pratt, Jr., J. Magn. Magn. Mater. **200**, 274 (1999).

[10] A.C. Reilly, W. Park, R. Slater, B. Ouaglal, R. Loloee, W.P. Pratt, Jr., and J. Bass, J. Magn. Magn. Mater. **195**, L269 (1999).

[11] I.A. Campbell and A. Fert, in *Ferromagnetic Materials*, edited by E.P. Wolforth (North-Holland, Amsterdam, 1982), Vol. 3, Chap. 9, p. 768.

[12] J.Z. Sun, J.C. Slonczewski, P.L. Trouilloud, D. Abraham, Ian Bacchus, W.J. Gallagher, J. Hummel, Yu Lu, G. Wright, S.S.P. Parkin, and R.H. Koch, Appl. Phys. Lett. **78**, 4004 (2001).

[13] J.Z. Sun, L. Chen, Y. Suzuki, S.S.P. Parkin, and R.H. Koch, J. Magn. Magn. Mater. **247**, L237 (2002).

[14] K. Inomata, N. Koike, T. Nozaki, S. Abe, and N. Tezuka, Appl. Phys. Lett. **82**, 2667 (2003).

[15] A. Girgis, J. Scheltem, J. Si, J. Janesky, S. Tehrani, and H. Goronkin, Appl. Phys. Lett. **76**, 3780 (2000).